ORIGINAL PAPER

Synthesis of Novel Fluorescent Cyclohexenone Derivatives and their Partitioning Study in Ionic Micellar Media

**Amir Badshah · Saleem Nawaz ·
Muhammad Faizan Nazar · Syed Sakhawat Shah ·
Aurangzeb Hasan**

Abstract An approach is demonstrated toward the synthesis of four novel cyclohexenone derivatives (CDs) *via* a convenient route of Michael addition of ethyl acetoacetate. The molecular structures of CDs were confirmed by means of FT-IR, ^{1}H NMR, EIMS, UV and also by X-ray single crystal structure analysis. CDs are strongly fluorescent compounds and their fluorescent spectra exhibits intense violet fluorescence. To model the binding to biological membranes the behavior of CDs in micellar solutions of a cationic surfactant, cetyltrimethylammonium bromide (CTAB) and an anionic surfactant, sodium dodecylsulfate (SDS) has also been examined. The characteristics of partition and binding interactions of CDs with CTAB and SDS were investigated by UV-Visible and fluorescence spectroscopic techniques. Higher values of all mentioned interactions in case of CTAB, compared to SDS, indicate that there are greater interactions between the CDs and CTAB than with SDS.

A. Badshah · S. Nawaz · M. F. Nazar (✉) · S. S. Shah · A. Hasan
Department of Chemistry, Quaid-i-Azam University,
45320 Islamabad, Pakistan
e-mail: faizan_qau@yahoo.com

M. F. Nazar
School of Chemistry, University of Bristol,
Bristol BS8 1TS, UK

Introduction

Consequently amplification of a large number of dyes and specific probe molecules has rapidly opened the window for luminescence probing techniques over the past three decades [1]. The design of new fluorescent probe molecules is a subject of intense research as they are valuable probes to explore the structural as well as functional aspects of biological systems [2]. Cyclic chalcones are carriers of different types of biological activity [3, 4]. The motive for their preparation is a variety of medical effects. Cyclohexenone carboxylates have known to possess anti-cancer [5], anti-HIV [6, 7], anti-fungal [8], anti-tumor [9, 10], anticonvulsant [11, 12] and antitubercular [13] activity. A series of novel compounds has been synthesized; known as cyclohexenoic long chain fatty alcohols, which are used in the treatment of neurological disorders [14]. From a chemical point of view, an important feature of chalcones is the ability to act as activated unsaturated systems in conjugated addition reactions of carbanions in the presence of basic catalysts [15, 16]. This type of reaction may be exploited for the preparation of 3,5-diaryl-6-carbethoxycyclohexenones *via* Michael addition of ethyl acetoacetate. The mentioned cyclohexenones are effective synthons in some projected synthesis of benzoselenadiazoles and benzothiadiazoles [17], spirocyclohexanones [18], carbazole derivatives [19], fused isoxazoles and pyrazoles [20, 21].

The synthesis of 5-aryl-6-carbethoxy-2-cyclohexenone substituted in position 3 with a 2-furanyl moiety through the Michael addition of ethyl acetoacetate to 3-aryl-1-(2-furanyl)-2-propenones has already been briefly described [22]. This paper presents the synthesis of some new 5-aryl-6-carbethoxy-3-(2-furanyl)-2-cyclohexenone, whose various chemical functions and optical properties commend them as valuable compounds for applications in violet-light-emitting devices (light emitting

laser, laser pointers, light-emitting diodes etc.) [23] or fluorescent dyes. Herein we report the synthesis of cyclohexenone derivatives and their photoluminescent properties.

The partitioning of cyclohexenone derivatives (CDs) was also studied quantitatively between the micelles and surrounding aqueous bulk. Conjugated cyclic enones react smoothly in water with a variety of aldehydes (Baylis-Hillman reaction) in the presence of surfactants above their critical micelle concentrations [24]. Efficient removal and sorption of 2-cyclohexenone to a benzyltrimethylammonium cation has also been developed [25]. The additive must partition to a well-defined and energetically favorable environment, orientation, and conformation in the membrane bilayers before diffusing into intrabilayer receptor binding cell [26]. The physical behavior of the surfactant micelles can be visualized as the construction of model membrane to mimic a biological system. The experimental model is useful for studying the interaction of biological surfaces with solubilizate [27, 28].

The aggregation behavior of surfactants-CDs in water was elucidated using simple UV-visible spectroscopy, differential UV-visible spectroscopy and Steady-state fluorescence spectroscopy (SSFS). By employing the above mentioned spectroscopic techniques, the micellar-water partition coefficient (K_x), the standard free energy change of solubilization (ΔG_P), the additive-surfactant binding constant (K_b), the binding energy (ΔG_b), the number of binding sites or binding capacity (n_b) and the number of additive molecules per micelle solution (n) have been calculated at 25 °C. The results point toward a strong partitioning of the cyclohexenone derivatives in favor of the micellar pseudo-phase.

Materials and methods

Reagents

The reagents; ethyl acetoacetate, 3-Bromobenzaldehyde, 2-Chlorobenzaldehyde, 4-Ethoxybezaldehyde, 3-Methoxybenzaldehyde were purchased from Fluka (Germany). The liquid reagents were distilled at their boiling points and the solid reagents were characterized by recording their melting points. No further purification was required. Sulphuric acid and hydrochloric acid (37%) were obtained from Stedee Ltd. The solvents chloroform, ethyl acetate, absolute ethanol and pet ether were purchased from Sigma Aldrich (Germany). All the solvents were used after necessary purification and drying according to the standard procedures. The dried solvents were stored over molecular sieves (4Å). Sodium dodecylsulphate (SDS) was 99% pure and was purchased from Fluka. Cetyltrimethylammonium bromide (CTAB) was purchased from Sigma Chemical Co.

Compound characterization techniques

R_f values were calculated by using precoated silica gel aluminum backed plates Kiesel gel 60F$_{254}$ Merck (Germany) using ethylacetate : pet-ether (1:4) as developing solvents. Melting points of the compounds were determined in open capillaries using Gallenkamp melting point apparatus and are uncorrected. The FTIR spectral data were recorded on Bio-Rad Merlin Spectrophotometer using KBr discs. ^{1}H NMR spectra were recorded on Bruker (300 MHz) AM-250 spectrometer in CDCl$_3$ solution using TMS as internal standard. EIMS was recorded on Agilent mass spectrometer. Purity of each compound was ascertained by thin layer chromatography. The purification of synthesized compounds was achieved mostly through recrystallization, the use of solvent extraction, or by making preparative thin layer chromatography or column chromatography whenever required.

Steady-state fluorescence measurements

Steady-state fluorescence (SSF) was performed on a Perkin Elmer LS 55 Luminescence Spectrometer with PC controlled software FinWinLab. The Photo Multiplier tube (PMT) voltage was kept at 665 V. The emission and excitation slits were fixed at 6.0 nm each. The excitation wavelength was taken as 331 nm. The scan range used was from 350–600 nm. Polarizers were kept clear and no cutoff was operating during the scan. The temperature of the cell was fixed with the help of an external circulator water bath.

Spectrophotometric (UV-visible) measurements

Spectrophotometric measurements were performed on a Perkin-Elmer Lambda 20 ultraviolet-visible spectrophotometer with 1.0 cm quartz cells at a temperature of 25.0±0.1 °C. Differential absorbance measurements were made in such a way that additive solution of a particular concentration was kept on the reference side and the surfactant-additive solution on the sample side in the spectrophotometer.

General synthetic methods

In view of the immense pharmacological and physiological importance of cyclohexenone, the present work was undertaken to synthesize this class of organic compounds with variable substituents to diversify in the ring of the chalcones. As such a variety of cyclohexenone derivatives were obtained in moderate to good yields. The synthetic strategy for the titled compounds is outlined in the following Scheme 1.

Furanyl-containing chalcone analog 1 (3 mmol) and ethyl acetoacetate 2 (0.39 g, 0.40 mL, 3 mmol) were
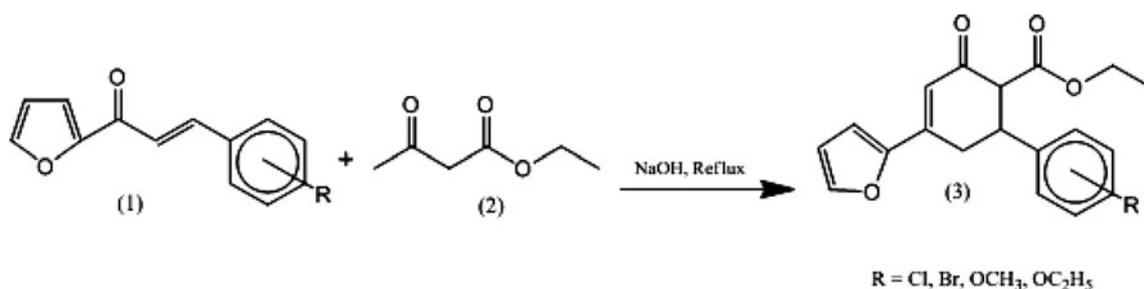
Scheme 1 General methodology for the synthesis of cyclohexenone derivatives

refluxed for 2 h in 10–15 mL ethanol in the presence of 0.5 mL 10% NaOH. The reaction mixture was then poured with good stirring into 200 mL ice-cold water and kept at room temperature until the reaction product separated as a solid, which was filtered off and recrystallized from ethanol.

Results and discussion

Synthesis of cyclohexenone

The reaction of chalcones and their heterocyclic analogs with ethyl acetoacetate in the presence of basic condition underwent Michael addition followed by internal claisen condensation to produce cyclohexenone, as outlined in Scheme 1.

The organic compounds were separated out by pouring the reaction mixture into water. All Compounds precipitated after being kept for several days. The solid products were separated by filtration, dried and recrystallized from ethanol. The yields of the cyclocondensation were good, varying from 63 to 70%. Structural analysis of the newly synthesized cyclohexenone was done by analytical and spectral data. The IR spectra of these compounds revealed a sharp strong absorption band around 1,730–1,740 cm^{-1} that can be correlated with the presence of the ester function in the structure of cyclohexenone. Furthermore, another sharp strong absorption band at around 1,650–1,660 cm^{-1} assigned to the conjugated carbonyl group. The bands at 2,900–3,100 cm^{-1} accounted for the OH group due to enol form and the hydrogen bonded carbonyl of ester group appeared around 1,500–1,600 cm^{-1}.

The ^{1}H-NMR spectra substantiated the results of the IR analysis. One of the representative compounds of cyclohexenone series, ethyl 6-(4-ethoxyphenyl)-4-(furan-2-yl)-2-oxocyclohex-3-ene-1-carboxylate (1FuE), has been described here in detail. In the ^{1}H-NMR spectrum of (1FuE), the ethyl protons resonated as a triplet and a quartet at 1.07 ppm 4.07 ppm integrating for three and two protons respectively. The characteristic signal in the ^{1}H NMR spectrum of compound (1FuE) is however the singlet of the vinylic proton in the position C-3 of the cyclohexenone rings, that occurs at approximately 6.61 ppm integrating for one proton, and confirms that the intramolecular cyclo-condensation subsequent to the Michael addition actually took place. The signal due to the C-5 methylene protons appeared as two doublets at 3.03 ppm and at 3.07 ppm respectively thereby indicating that they are diastereo-tropic protons. The signal due to C6-H appeared as a multiplet centered at 2.83 ppm integrating for one proton. The C1-H proton appeared as doublet at 3.73 ppm integrating for one proton. As for the protons in the aromatic region, the ^{1}HNMR spectrum allowed the assignments of the protons in the furane ring at 6.53 ppm, 6.85 ppm and 7.23 ppm. The number of the other aromatic protons of the aryl substituent in the C-6 of the cyclo-hexenone ring that was integrated in the ^{1}H NMR spectra of compound (1FuE) was always in good agreement with the factual one.

The mass spectrum of (1FuE) is also in accordance with the proposed structure showed characteristic peaks; however, the molecular ion peak is absent. The fragment peak at m/z 282 is due to the loss of ester moiety. The base peak appeared at m/z 134 as a result of Retro-Diels-Alder fission of cyclohexene ring. The peaks appeared at m/z 254 and 209 due to the loss of carbon monoxide molecule and then side chain respectively.

To understand their real structures [29], the single crystal of compound (1FuE) is determined by single-crystal X-ray diffraction. The molecular structure and packing diagram (Fig. 1) are discussed with their structural features, while their selected bond lengths and bond angles are shown in Table 1.

The synthetic procedure used for the synthesis of (1FuE) was also used for the synthesis of other members of the series. The molar ratio, physical, FTIR, ^{1}H NMR and EIMS data for these compounds are given below:

Ethyl-6-(3-bromophenyl)-4-(furan-2-yl)-2-oxocyclohex-3-ene-1-carboxylate (1FuB) Golden solid, Yield 2.85 g (63%); m.p.: 87–89 °C. ^{1}H NMR (CDCl$_3$, 300 MHz): δ 1.08 (t, J=7.2 Hz, 3H), 4.07 (q, J=7.2 Hz, 2H), 3.02 (dd, J_1=2.4 Hz, J_2=17.0, 1H), 2.79–2.87 (m, 1H), 3.73 (dd J_1=
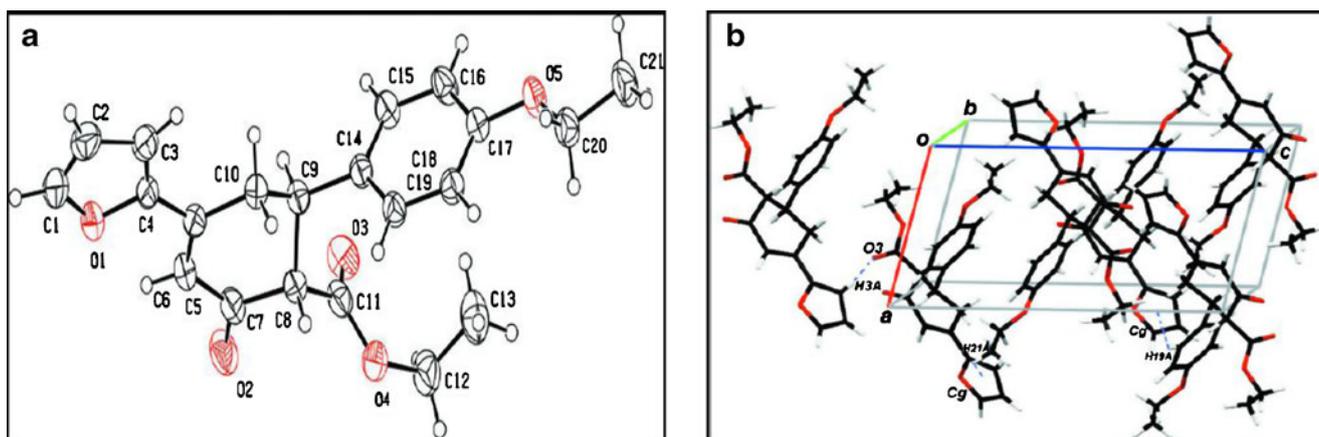
Fig. 1 X-ray Molecular structure of (1FuE). The displacement ellipsoids are drawn at the 40% probability level and the H atoms are shown as small spheres of arbitrary radii, (b) The packing diagram of the (1FuE), viewed along the *a*-axis showing the weak hydrogen-bond and C—H π electron interactions

2.8 Hz, J_2=6.70, 2H), 6.61 (s, 1H), 7.58 (d, *J*=1.8 Hz, 1H), 6.54 (dd J_1=1.8 Hz, J_2=3.3, 1H), 6.77 (d, *J*=3.6 Hz, 1H), 7.23–7.42 (m, 4H). IR (KBr, cm^{-1}): 639, 1552, 1609, 1666, 1725, 2993. MS (EI): *m/z* (%) = 318(25), 134(100), 106 (20), 51(5), 39(4), 290(3), 209(2).

Ethyl-6-(2-chlorophenyl)-4-(furan-2-yl)-2-oxocyclohex-3-ene-1-carboxylate (1FuC) Beige solid, Yield 3.1 g (67%); m.p.: 116–118 °C. ^{1}H NMR (CDCl$_3$, 300 MHz): δ 1.07 (t, *J*=7.1 Hz, 3H), 4.07 (q, *J*=7.1 Hz, 2H), 3.08 (dd, J_1= 2.6 Hz, J_2=17.5, 1H), 2.75–2.82 (m, 1H), 3.79 (dd J_1= 2.9 Hz, J_2=6.9, 2H), 6.62 (s, 1H), 7.58 (d, *J*=1.5 Hz, 1H), 6.54 (dd J_1=1.8 Hz, J_2=3.3, 1H), 6.78 (d, *J*=3.8 Hz, 1H), 7.20–7.44 (m, 4H). IR (KBr, cm^{-1}): 750, 1512, 1600, 1652, 1736, 2978. MS (EI): *m/z* (%) = 272(33), 134(100), 106 (20), 51(7), 39(5), 244(2), 209(2).

Ethyl 6-(4-ethoxyphenyl)-4-(furan-2-yl)-2-oxocyclohex-3-ene-1-carboxylate (1FuE) Bright yellow solid, Yield 3.3 g

Table 1 Selected bond lengths (Å) and angles (deg) for compound 1FuE

Bond lengths			
O1—C1	1.353 (2)	O1—C4	1.3642 (16)
O2—C7	1.2186 (17)	O3—C11	1.1949 (18)
O4—C11	1.3157 (18)	O4—C12	1.4449 (18)
O5—C17	1.3616 (15)	O5—C20	1.4164 (17)
C4—C5	1.4367 (19)	C8—C11	1.5090 (19)
C9—C14	1.5095 (17)		
Bond angles			
C6—C5—C4	121.59 (12)	C6—C5—C10	121.65 (12)
C11—C8—C7	111.43 (11)	C11—C8—C9	110.98 (11)
C14—C9—C10	114.30 (10)	C14—C9—C8	112.04 (10)
O5—C17—C16	116.00 (11)	O5—C17—C18	124.71 (11)
C19—C14—C9	122.46 (11)	C15—C14—C9	120.24 (11)

(70%); m.p.: 114–116 °C. ^{1}H NMR (CDCl$_3$, 300 MHz): δ 1.07 (t, *J*=7.2 Hz, 3H), 4.07 (q, *J*=6.9 Hz, 2H), 3.03 (dd, J_1=3.0 Hz, J_2=18.0, 1H), 2.72–2.81 (m, 1H), 3.72 (dd J_1= 2.7 Hz, J_2=6.75, 2H), 6.60 (s, 1H), 7.57 (d, *J*=1.5 Hz, 1H), 6.53 (dd J_1=1.8 Hz, J_2=3.4, 1H), 6.75 (d, *J*=3.6 Hz, 1H), 6.85 (dd J_1=2.1 Hz, J_2=6.6, 2H), 7.23 (dd J_1=3.0 Hz, J_2= 6.6, 2H), 1.43 (t, *J*=7.2 Hz, 3H), 4.09 (q, *J*=7.1 Hz, 2H). IR (KBr, cm^{-1}): 1038, 1510, 1604, 1657, 1729, 2977. MS (EI): *m/z* (%) = 282(33), 134(100), 106(10), 51(6), 39(5), 254(12), 209(2), 119(60), 91(10), 65(3).

Ethyl 6-(3-methoxyphenyl)-4-(furan-2-yl)-2-oxocyclohex-3-ene-1-carboxylate (1FuM) Orange solid, Yield 3.0 g (65%); m.p.: 82–84 °C. ^{1}H NMR (CDCl$_3$, 300 MHz): δ 1.07 (t, *J*=7.0 Hz, 3H), 4.09 (q, *J*=6.9 Hz, 2H), 3.00 (dd, J_1=2.7 Hz, J_2=17.0, 1H), 2.81–2.87 (m, 1H), 3.74 (dd J_1= 2.8 Hz, J_2=6.2, 2H), 6.60 (s, 1H), 7.57 (d, *J*=1.7 Hz, 1H), 6.53 (dd J_1=1.8 Hz, J_2=3.4, 1H), 6.77 (d, *J*=3.6 Hz, 1H), 6.99–7.25 (m, 4H), 3.81 (s, 3H). IR (KBr, cm^{-1}): 1050, 1523, 1603, 1658, 1729, 2980. MS (EI): *m/z* (%) = 268(30), 134(100), 106(5), 51(4), 39(4), 240(5), 209(3), 119(12), 91 (10), 65(3).

On the basis of the aforementioned results the structures of cyclohexenone derivatives are as follows (Table 2):

Absorption and emission spectra of cyclohexenone derivatives

The UV-Visible absorption spectra and fluorescence emission spectra of cyclohexenone derivatives are shown in Fig. 2. The absorptions of cyclohexenone derivatives were located at 331 nm. Their excitation wavelengths were all fixed at 331 nm. It is found that their intensity of fluorescence differs from each other but shows the same emission maximum (λ_{em}) of 412 nm in the violet region.

Table 2 Structures and R_f values of cyclohexenone derivatives

Compound	Structure	Molecular Formula	Molecular Weight	[a]R_f Values x 100
1FuB		$C_{19}H_{17}BrO_4$	389	67
1FuC		$C_{19}H_{17}ClO_4$	344.8	62
1FuE		$C_{21}H_{22}O_5$	354.4	57
1FuM		$C_{20}H_{20}O_5$	340.4	54
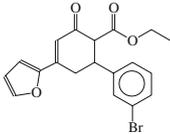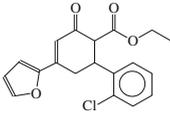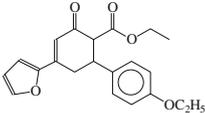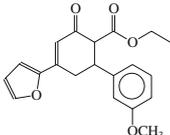
[a]**Solvent for R_f values = Pet-ether:ethylacetae (4:1)**

Interactions of cyclohexenone derivatives with ionic surfactants

UV visible absorption spectroscopy

Simple absorption spectra of cyclohexenone derivatives (CDs) with varying concentration of surfactants (SDS and CTAB) give some useful information about the interaction of CDs and the surfactant. Figure 3 shows the simple absorbance spectra of one of the representative compound of cyclohexenone series (1FuE) with varying concentration of surfactants i.e. SDS (0.006 mol.dm^{-3} to 0.02 mol.dm^{-3}) and CTAB (0.0006 mol.dm^{-3} to 0.002 mol.dm^{-3}). The absorbance of 1FuE increases with increasing concentration of surfactants. The interaction between additive and the surfactants below CMC allow the additive to absorb light more favorably; hence absorbance is enhanced in the sub-micellar region. The leveling off the curve above CMC shows the maximum solubilization of additive molecules within the micelle.

The increase in absorbance at micellar concentration is due to the tendency of hydrophobic additive molecules to enter into the micelle. Although the additive molecules are incorporated in the micelles, their chromophores are still oriented near the surface and hence absorb light more favorably than in the aqueous bulk solution [30]. The micellar interior is a nonpolar moiety where the aqueous bulk is a polar. So the hydrophobic 1FuE molecules prefer to reside inside or near the nonpolar core of the micelle. After micelle formation the absorbance of the system become constant on further addition of surfactants (Inset of Fig. 3).

CDs-micelle interaction is better explained by quantifying their magnitude through the elucidation of additive-micelle partition coefficient (K_x), the standard free energy of solubilization (ΔG_p) of the additive in micelles, the additive-surfactant binding constant (K_b), the binding energy (ΔG_b), the number of binding sites or binding capacity (n_b) and the number of additive molecules in a micelle solution (n). In case where interactions of the molecule with its surrounding environment are intrinsically related to spectral characteristics, their changes can be used for the determination of corresponding partition coefficients and approximate numbers of dye molecules per micelle.
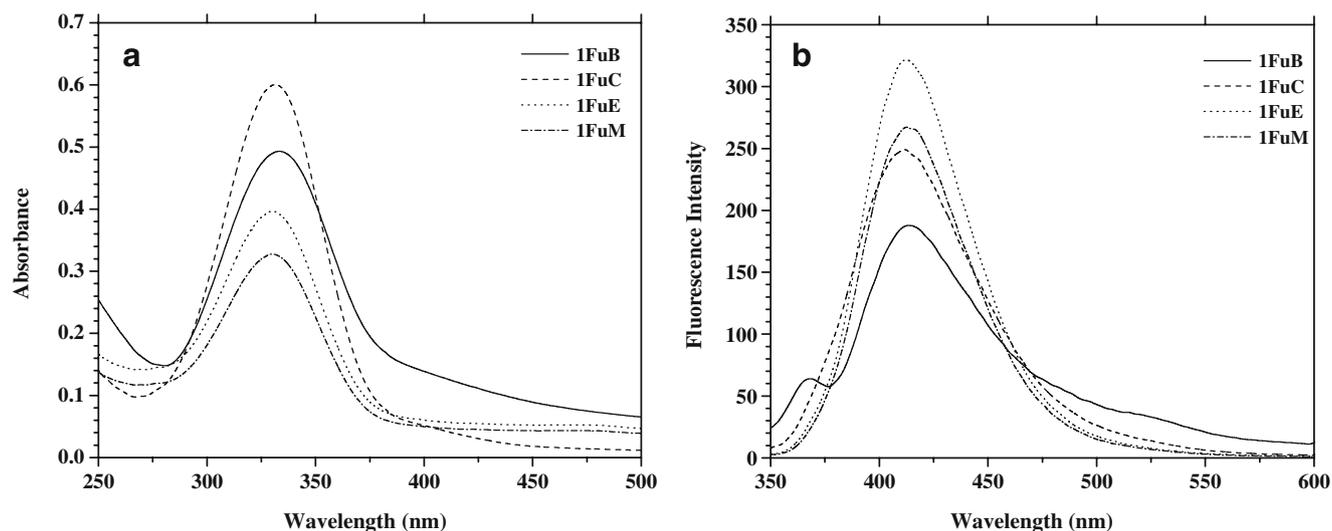
Fig. 2 Spectra of aqueous solution (3% ethanol) of cyclohexenone derivatives with the concentration of 3×10^{-5} M; **a** The normalized absorption spectra **b** The emission spectra

The approximate number of additive molecules incorporated into a single micelle (n) is calculated by using the following relations [30, 31]. Results of all the cyclohexenone derivatives (CDs) are shown in Table 3.

$$n = \frac{C_m}{M} \tag{1}$$

and

$$M = \frac{C_s - CMC}{N} \tag{2}$$

Here C_m is the concentration of additive solubilized in the micelle, M is the micelle concentration, C_s is the total surfactant concentration and N is the mean aggregation number of micelles at CMC in water. The normal CMCs of the CTAB and SDS are 0.9 mM and 8.2 mM respectively [32]. C_m is the concentration of solubilized additive, which is determined, as [33]:

$$C_m = \frac{A_o - A}{\varepsilon_o - \varepsilon_m} \tag{3}$$

Here A_o is the absorbance of additive solution in the absence of surfactant, A is the absorbance at any point in the presence of surfactant above the CMC, ε_o is calculated from A_o, and ε_m is determined at higher surfactant concentration above the CMC when the absorbance of the additive-
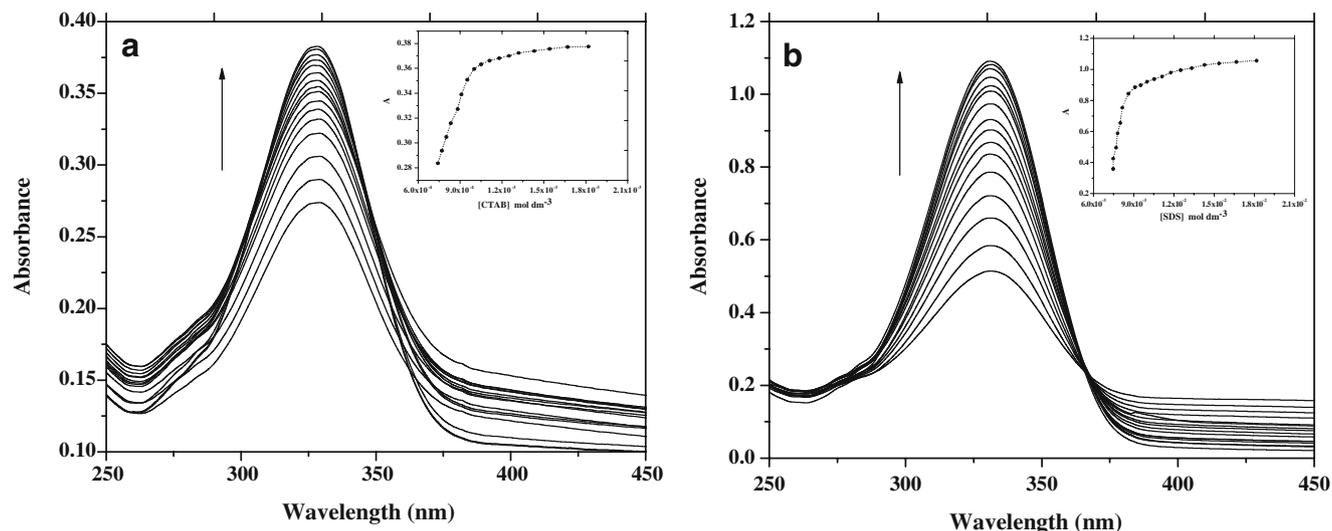
Fig. 3 Simple absorbance spectra of 1FuE with varying concentration of surfactants in aqueous solution at 25 °C, **a** CTAB **b** SDS. Arrow indicates change in absorbance of 1FuE with increasing surfactants

concentration. *Inset*: Relation between absorbance of (Surfactants + additive) and concentration of surfactants

Table 3 Calculation of n, K_c, K_x and ΔG_p for cyclohexenone derivatives in micellar solution of ionic surfactants

Surfactant	Compound	$n = C_m/M$	K_c (dm³mol⁻¹)	K_x	ΔG_p (kJ/mol)
CTAB	1FuB	4	2.50×10^3	1.39×10^5	−29.34
	1FuC	6	4.21×10^3	2.34×10^5	−30.63
	1FuE	6	4.88×10^3	2.71×10^5	−30.99
	1FuM	5	3.60×10^3	2.00×10^5	−30.24
SDS	1FuB	1	3.73×10^2	2.07×10^4	−24.62
	1FuC	1	5.19×10^2	2.88×10^4	−25.44
	1FuE	1	7.21×10^2	4.01×10^4	−26.26
	1FuM	1	4.16×10^2	2.31×10^4	−24.89

surfactant solution becomes almost constant. The micellar aggregation number used for CTAB is 80 and for SDS it is 70 [34]. For a particular concentration of CTAB (C_s), higher value of 'n' shows the more hydrophobicity of CDs in aqueous solution than for SDS.

Differential absorbance spectra of 1FUE with CTAB

Differential spectroscopy technique was utilized to study the partitioning of cyclohexenone derivatives from aqueous to the micellar environment. Partition coefficient (K_x) results are intrinsically valuable providing essential data relating to the interactions of organic solubilizate with the surfactant micelles and the locus of solubilizate within the micelles.

Figure 4 shows the differential absorption spectra of the additive (1FuE) in presence of various concentrations of surfactants (CTAB and SDS) independently at 25 °C. No shift in the peaks was observed. The mounting value of ΔA with increasing surfactant concentration can be seen in connection to the increase in 1FuE molecules solubilized by the micelles.

Solubilized additive molecules thus distribute themselves according to their polarity between the highly

nonpolar central region and the relatively polar interfacial region of the micelles [35, 36]. The partitioning of the additive molecules in water micelle system is calculated using equation proposed by Kawamura et al. [37]. The equation is given as:

$$\frac{1}{\Delta A} = \frac{1}{K_c \Delta A_\infty \left(C_a + C_s^{mo}\right)} + \frac{1}{\Delta A_\infty} \tag{4}$$

Where C_a is the additive concentration, C_s^{mo} represents C_s-CMC_0 (CMC_0 is the CMC of surfactant in water), ΔA_∞ is the differential absorbance at the infinity of C_s. K_c can be obtained through intercept and slope values of the straight line plot of $1/\Delta A$ against $1/\left(C_a + C_s^{mo}\right)$, as shown in Fig. 5. The value of K_c is given in Table 3.

The dimensionless partition coefficient K_x is related to K_c as $K_x = K_c.n_w$, where n_w is the number of moles of water per dm³ (55.55 mol dm⁻³), and is reported in Table 3. The standard free energy change of the transfer (ΔG_p) of additive from bulk water to micelle can be calculated using the following relation:

$$\Delta G_p = -RT \ln K_x \tag{5}$$
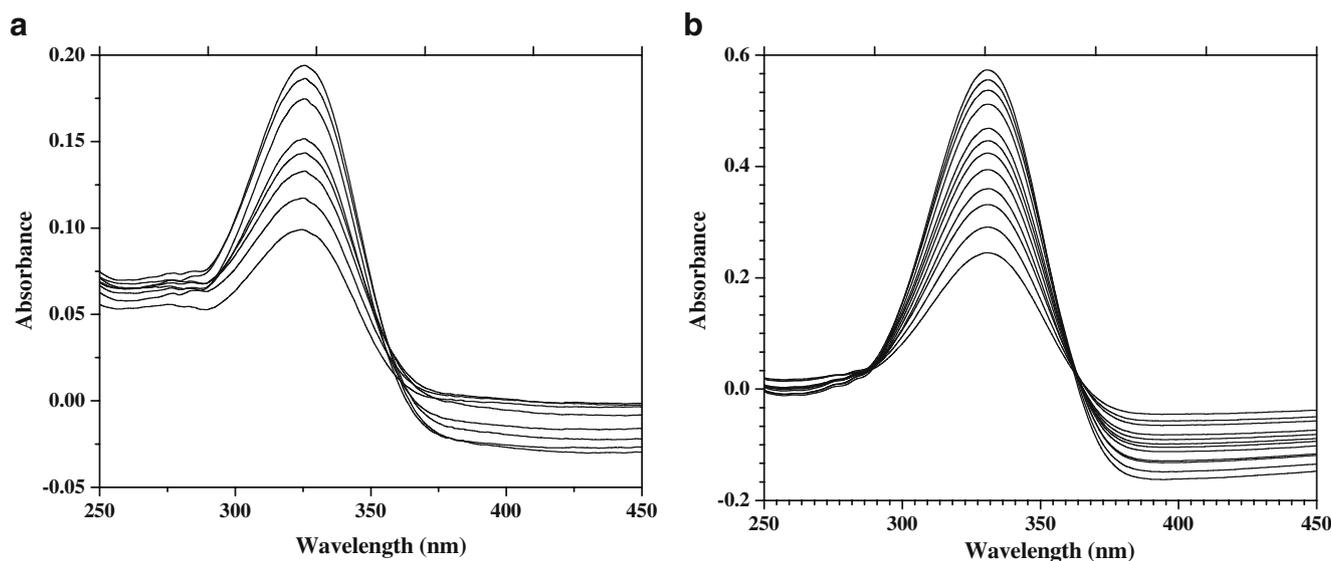
Fig. 4 Differential absorbance spectra of 1FuE with changing concentration of surfactants. **a** CTAB, **b** SDS
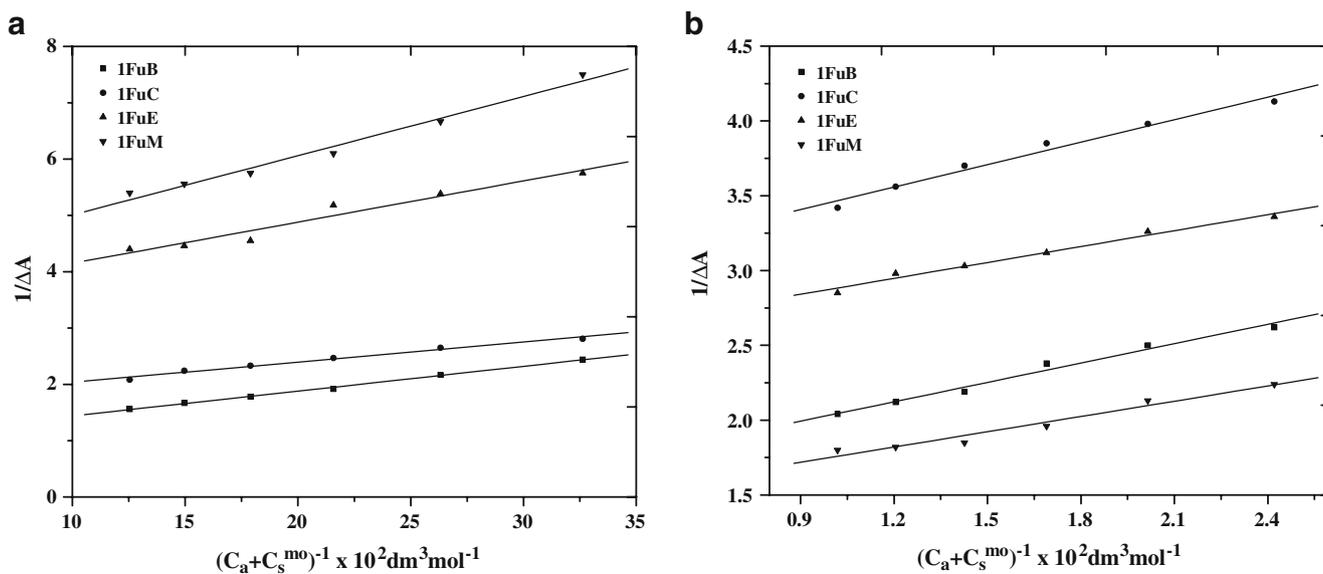
Fig. 5 Plot of inverse of differential absorbance ($1/\Delta A$) vs. $(C_a + C_s^{mo})^{-1}$ of all the cyclohexenone derivatives and concentration of surfactants, **a** CTAB, **b** SDS

Here T is absolute temperature and R is the gas constant. The values of K_c, K_x and ΔG_p of all the cyclohexenones derivatives (CDs) are reported in Table 3. The negative ΔG_p value implies that the process of the additives partition is a spontaneous one [38]. This can be justified due to the hydrophobic nature of the cyclohexenone derivatives. Different parameters obtained from spectroscopic measurements indicate enhanced solubility of the cyclohexenones derivatives in the micellar region. The increases in K_x values with hydrophobicity of additive molecules indicate that mainly the hydrophobic interactions between the additives

and the micelles control the solubilization. From the high negative value of ΔG_p it can be concluded that although some interaction with the polar surface of the micelle is possible but the most favored place is toward the micellar core.

Steady-state fluorescence spectroscopy study

Fluorescence emission spectroscopy is utilized to study the interaction of cyclohexenone derivatives (CDs) with ionic surfactants. Fluorescence measurements can give some information on the binding of additive molecules to the
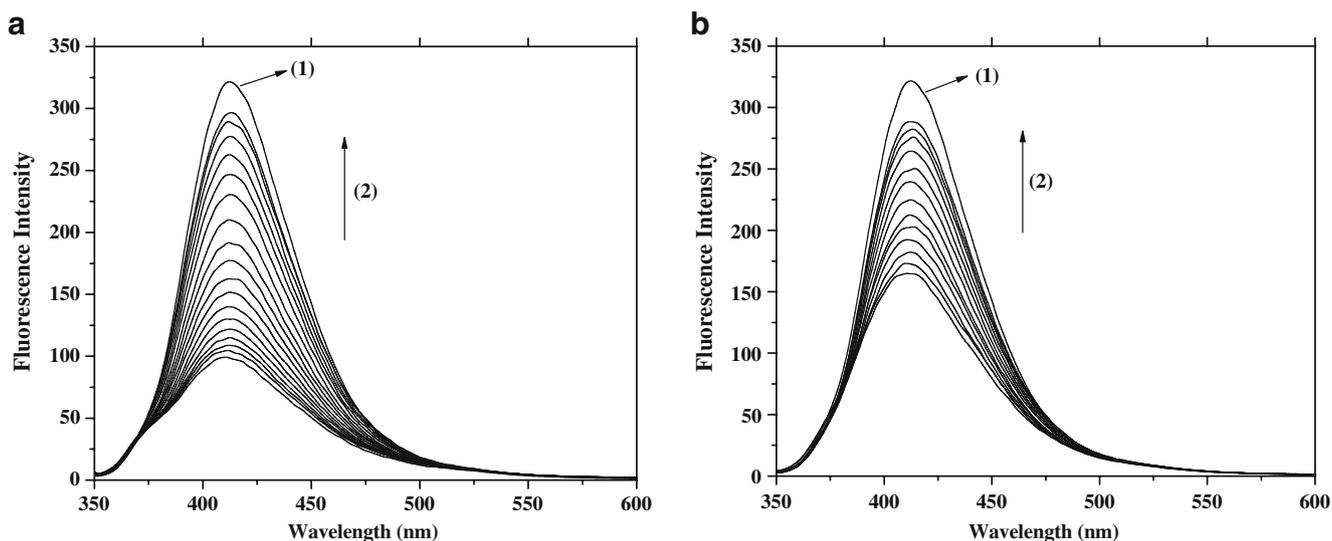
Fig. 6 Fluorescence emission spectra of 1FuE at varying concentration of surfactants; **a** CTAB, **b** SDS. (1) Fluorescence intensity of pure 1FuE, (2) Arrow indicates that fluorescence intensity of 1FuE increases with decreasing surfactants concentration
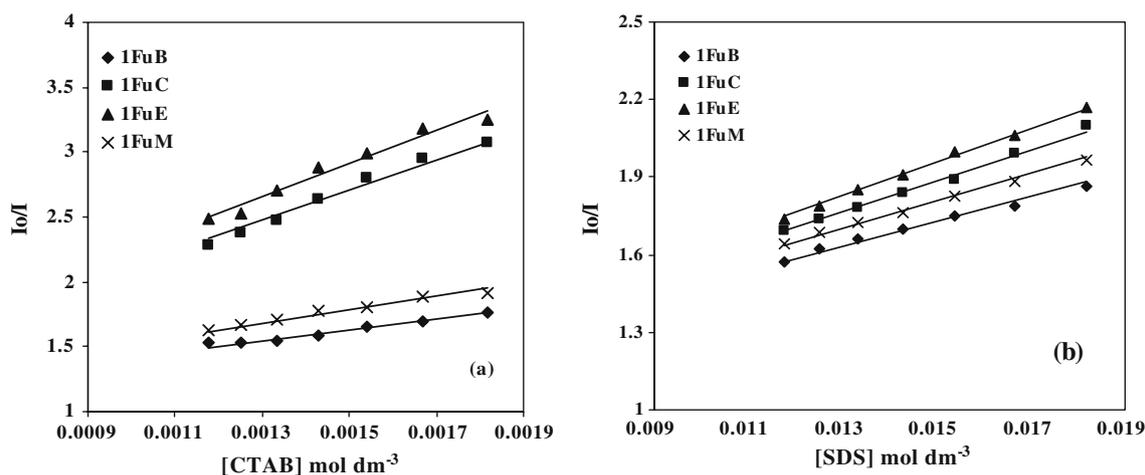
Fig. 7 Stern-Volmer plot for the binding of all the cyclohexenone derivatives with surfactants; a CTAB, b SDS

surfactants, such as the binding constants and the number of binding sites [39]. Fluorescence intensity of a compound can be decreased by a variety of molecular interactions, viz., excited-state reactions, molecular rearrangements, energy transfer, ground state complex formation and collisional quenching. Such a decrease in intensity is called quenching [40]. Fluorescence spectra of cyclohexenone derivatives (CDs) in the presence of different amounts of surfactants (CTAB and SDS) were recorded in the range of 350–600 nm upon excitation at 331 nm.

CTAB and SDS both caused a concentration-dependent quenching of the intrinsic fluorescence of cyclohexenone derivatives (CDs). Figure 6 indicated that there were interactions between 1FuE and surfactants and the binding resulted in a non-fluorescent complex without changing the emission maximum.

The fluorescence quenching data was analyzed by the Stern-Volmer equation:

$$I_o/I = 1 + K_{sv}[Cs] \qquad (6)$$

Where I_o and I are the steady-state fluorescence intensities in the absence and presence of quencher (surfactants), respectively, K_{sv} the Stern-Volmer quenching

constant and [Cs] is the concentration of surfactants (CTAB and SDS) independently. Stern-Volmer plot (I_o/I versus [Cs]) for all the cyclohexenone derivatives (Fig. 7) revealed the quenching type, may be static or dynamic, since the characteristic Stern-Volmer plot of combined quenching (both static and dynamic) is an upward curve (as in the Fig. 7). The values of K_{sv} of all the cyclohexenones derivatives (CDs) are shown in Table 4.

Analysis of binding equilibria

The above results indicate that both surfactants (CTAB and SDS) act as a quencher in its interaction with cyclohexenone derivatives. The binding constant and binding affinities were calculated using following equation [41]:

$$\log\left[(Io - I)/I\right] = \log K_b + n_b \log[Cs] \qquad (7)$$

Where K_b is binding constant and n_b is number of binding sites or binding capacity. I_o and I represent the fluorescence intensities of the cyclohexenone derivatives in the absence and presence of surfactants, respectively. Plotting log [(Io-I)/I] versus log [Cs] gives rise to n_b (from slope) and log K_b (from intercept) as shown in Fig. 8.

Table 4 Calculation of n_b, K_b, K_{sv} and ΔG_b for cyclohexenone derivatives in micellar solution of ionic surfactants

Surfactant	Compound	n_b	log K_b	K_b (dm³mol⁻¹)	ΔG_b (kJ/mol)	K_{sv} (dm³mol⁻¹)
CTAB	1FuB	1.66	4.51	3.24×10^4	−25.73	4.21×10^2
	1FuC	1.63	4.74	5.49×10^4	−27.04	11.40×10^2
	1FuE	1.64	4.85	7.08×10^4	−27.67	12.75×10^2
	1FuM	1.67	4.60	3.98×10^4	−26.24	5.27×10^2
SDS	1FuB	1.36	2.45	2.82×10^2	−13.98	4.84×10^1
	1FuC	1.39	2.51	3.24×10^2	−14.32	5.91×10^1
	1FuE	1.43	2.52	3.31×10^2	−14.38	6.38×10^1
	1FuM	1.44	2.48	3.02×10^2	−14.15	5.38×10^1

a

b
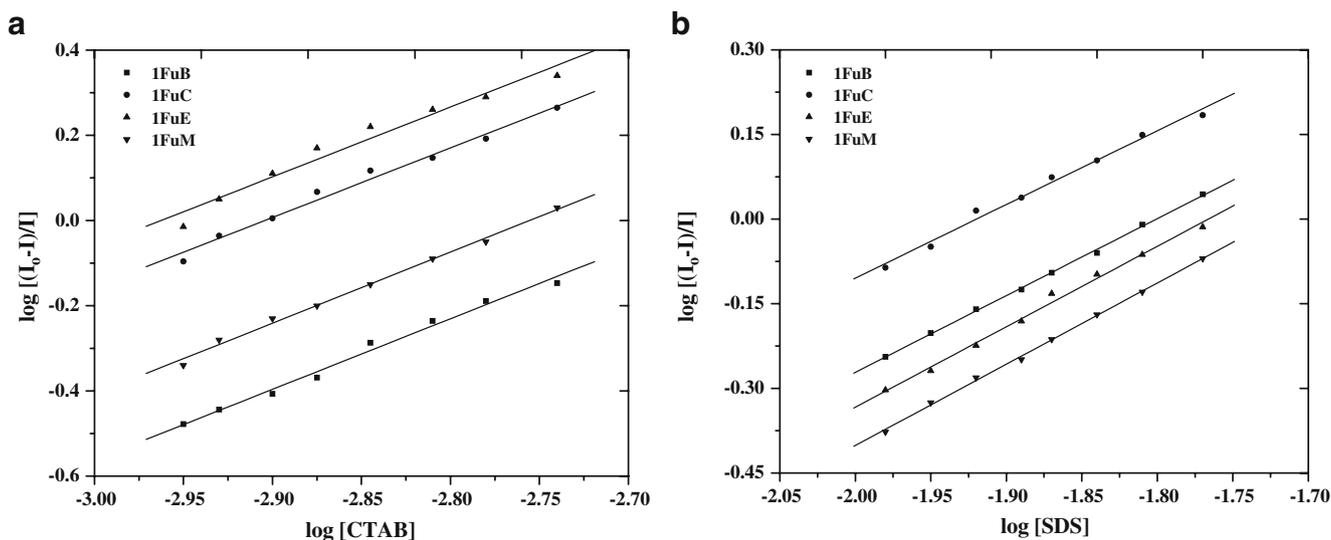
Fig. 8 The plot for binding constant and binding sites of all cyclohexenone derivatives with surfactants; **a** CTAB, **b** SDS

The binding constant (K_b) thus obtained was used to calculate the standard free energy change ΔG_b of the additive binding to surfactants from the following relationship:

$$\Delta G_b = -RT \ln K_b \tag{8}$$

The values of binding constant K_b, binding energy ΔG_b and binding capacity n_b thus determined were listed in Table 4. The values of K_b are comparable. High values of K_b indicate that the interactions between cyclohexenone derivatives and CTAB are strong compared to SDS.

From the result it is also clear that all the four compounds showed almost similar results in both cases of SDS and CTAB. This may be due to the fact that the substituents present are away from the binding sites and affect the interactions very little. The smaller n_b values of SDS, compared to CTAB, indicate that there are less binding sites available for it to bind cyclohexenone derivatives. This may be due to the fact that the SDS micellar surface is negatively charged and that of CTAB is positively charged while there is an electron system in the cyclohexenone derivatives. So in the case of CTAB there may be more electrostatic interactions present, compared to SDS, besides hydrophobic interactions.

Conclusion

The present work has described the synthesis and photoluminescent properties of a new fluorescent series of cyclohexenone derivatives. These compounds could function as environment sensitive fluorescent probes and their expanded applications to biological samples for membrane solubilization properties and in drug delivery events are expected. This present work has also provided a good example about how to increase the solubility of water-insoluble drugs, to enhance their loading efficiency and to optimize the dispersion in drug carriers. Demanding effort has been made to differentiate assemblies such as micelles, vesicles, liposomes, microemulsions, polymers, and biological membranes over the past decades. Cyclohexenone derivatives are carriers of different types of biological activity. Their partitioning study of solubilized system can provide a useful insight into the process of solubilization, which is applicable to the general problem of membrane solubilization properties and in drug delivery to quantify the degree of drug-micelle interaction.

The interaction of reported cyclohexenone with ionic surfactants was investigated by UV-Visible and fluorescence spectroscopic techniques. Fluorescence intensity of cyclohexenone derivatives at 412 nm dropped regularly with the increasing concentrations of the surfactants resulted in a non-fluorescent complex without changing the emission maximum. Higher values of binding constant, quenching constant, numbers of binding sites and binding energy in case of CTAB, compared to SDS, indicate that there are more interactions between the cyclohexenone derivatives and CTAB than with SDS. It is clear from the discussion above that the cyclohexenone partitions strongly into the nonpolar environment. The results obtained from both UV-Visible and fluorescence spectroscopies support each other.

References

1. Mohr A, Talbiersky P, Korth HG, Sustmann R, Boese R, Blaser D, Rehage H (2007) A new pyrene-based fluorescent probe for the determination of critical micelle concentrations. J Phys Chem B 111:12985–12992

2. Hirano J, Hamase K, Akita T, Zaitsu K (2008) Structural and photophysical properties of novel dual fluorescent compounds, 1-aryl-substituted 6-methoxy-4-quinolones. Luminescence 23:350–355

3. Hayakawa K, Ohsuki S, Kanematsu K (1986) General approach for the stereocontrolled synthesis of tricyclic lactones via allene intramolecular cycloaddition. An application to the synthesis of (±)-platyphyllide. Tetrahedron Lett 27:947–950

4. Mori K, Kato M (1986) Synthesis and absolute configuration of (+)-hernandulcin. A new sesquiterpene with intensely sweet taste. Tetrahedron Lett 27:981–982

5. Zhi L, Martinborough E (2001) Selective androgen receptor modulators (SARMs). Ann Rep Med Chem 36:169–180

6. Bringmann G, Lang G, Muhlbacher J, Schaumann K, Steffens S, Rytik PG, Hentschel U (2003) Sorbicillactone A, a structurally unprecedented bioactive novel-type alkaloid from a sponge-derived fungus. Marine Mol Biotech 1:231–253

7. Bringmann G, Lang G, Muhlbacher J, Schaumann K, Steffens S, Muller WEG (2002) Method for producing sorbicillactone A. German Patent Application. (DE. 102 38 257.3)

8. Kong C, Xu X, Zhou B, Hu F, Zhang C, Zhang M (2004) Two compounds from allelopathic rice accession and their inhibitory activity on weeds and fungal pathogens. Phytochem 65:1123–1128

9. Stang PJ, Treptow WL (1981) Synthesis and biological activity of simple vinyl and methylene butyrolactone sulfonate esters and silyl enol ethers. J Med Chem 24:468–472

10. Li JY, Strobel GA (2001) Jesterone and hydroxy-jesterone antioomycetcyclohexenenone epoxides from the endophytic fungus. Phytochem 57:261–265

11. Nagarajan K, David J, Shah RK (1976) Central nervous system active 5-oxo-1, 4, 5, 6, 7, 8-hexahydrocinnolines. J Med Chem 19:508–511

12. Eddington ND, Cox DS, Roberts RR, Stables JP, Powell CB, Scott AR (2000) Enaminones-versatile therapeutic pharmacophores. Further advances. Curr Med Chem 7:417–436

13. Kachhadia VV, Popat KH, Nimavat KS, Joshi HS (2004) Synthesis, antitubercular and antimicrobial activity of 6-carbethoxy-5-aryl-3-[p-(3′-chloro-2′-benzo [b]thiophenoylamino) phenyl]-2-cyclohexenones. J Indian Chem Soc 81:694–695

14. Luu B, Aguilar JLGD, Junges CG (2000) Cyclohexenonic long-chain fatty alcohols as neuronal growth stimulators. Molecules 5:1439–1460

15. House HO (1972) Modern synthetic reactions. Benjamin WA, Menlo Park

16. Jung ME (1991) In: Trost BM, Fleming I (eds) Comprehensive organic synthesis. Pergamon, Oxford

17. Reddy DB, Reddy AS, Padmavathi V (1998) Synthesis of annelated 1,2,3-selena- or -thia-diazoles. J Chem Research (S) 784–785

18. Padmavathi V, Sharmila K, Reddy AS, Reddy DB (2001) Synthesis of spirocyclohexanones. Indian J Chem Sect B 40:11–14

19. Padmavathi V, Sharmila K, Padmaja A, Reddy DB (1999) An efficient synthesis of 6, 8-diarylcarbazoles via Fischer indole cyclizations. Heterocycl Commun 5:451–456

20. Padmavathi V, Reddy BJM, Balaiah A, Venugopal K, Reddy DB (2000) Synthesis of some fused pyrazoles and isoxazoles. Molecules 5:1281–1286

21. Padmavathi V, Sharmila K, Balaiah A, Reddy AS, Reddy DB (2001) Cyclohexenone carboxylates. A versatile source for fused isoxazoles and pyrazoles. Synth Commun 31:2119–2126

22. Usova EB, Lysenko LI, Krapivin GD, Kulnevich VG (1997) Furylcyclohexenones. Conversion of 6-ethoxycarbonylcyclohexenones into 4, 5-dihydroindazoles. Molecular and crystal structure of 4-phenyl-6-(5-methyl-2-furyl)-4, 5-dihydroindazol-3-one. Chem Heterocycl Compd 33:1259–1265

23. Sreevidya TV, Narayana B, Yathirajan HS (2010) Synthesis and characterization of some chalcones and their cyclohexenone derivatives. Cent Eur J Chem 8:174–181

24. Porzelle A, Williams CM, Schwartz BD, Gentle IR (2005) Evaluating the Baylis-Hillman reaction of cyclic enones using surfactants in water. Synlett 19:2923–2926

25. Zhu L, Ruan X, Chen B, Zhu R (2008) Efficient removal and mechanisms of water soluble aromatic contaminants by a reduced-charge bentonite modified with benzyltrimethyl-ammonium cation. Chemosphere 70:1987–1994

26. Rodrigues C, Gameiro P, Reis S, Lima J, de Castro B (2002) Interaction of grepafloxacin with large unilamellar liposomes: partition and fluorescence studies reveal the importance of charge interactions. Langmuir 18:10231–10236

27. Schreier S, Malheiros SVP, de Paula E (2000) Surface active drugs: self-association and interaction with membranes and surfactants, Physicochemical and biological aspects. Biochim Biophys Acta 1508:210–234

28. Kim EJ, Shah DO (2002) Cloud point phenomenon in amphiphilic drug solutions. Langmuir 18:10105–10108

29. Badshah A, Hasan A, Barbarie CR, Abbas A, Ali S (2009) Ethyl 6-(4-ethoxyphenyl)-4-(furan-2-yl)-2-oxocyclohex-3-ene-1-carboxylate. Acta Cryst E65, o70. doi:10.1107/S1600536808040130

30. Miyashita Y, Hayano S (1981) Kinetic study of the penetration of an anthraquinoid acidic dye into cationic micelles. Bull Chem Soc Jpn 54:3249–3252

31. Wang L, Verrall RE (1994) Apparent molar volume and apparent molar adiabatic compressibility studies of anesthetic molecules in aqueous micelle solutions of CTAB and CTAC as a function of surfactant concentration and temperature. J Phy Chem 98:4368–4374

32. Khamis M, Bulos B (2005) Azo dyes interactions with surfactants, Determination of the critical micelle concentration from acid-base equilibrium. Dyes Pigments 66:179–183

33. Khan AM, Shah SS (2008) A UV-visible study of partitioning of pyrene in an anionic surfactant sodium dodecyl sulfate. J Disp Sci Technol 29:1401–1407

34. Bahri MA, Hoebeke M, Grammenos A, Delanaye L, Vandewalle N, Seret A (2006) Investigation of SDS, DTAB and CTAB micelle microviscosities by electron spin resonance. Colloids Surf A 290:206–212

35. Rosen MJ (2004) Surfactants and interfacial phenomena. Wiley, New Jersey

36. Elworthy PH, Florence AT, Macfarlane CB (1968) Solubilization by surface-active agent. Champman and Hall, London

37. Kawamura H, Manabe M, Miyamoto Y, Fujita Y, Tokunaga S (1989) Partition coefficients of homologous phenylalkanols between water and sodium dodecyl sulfate micelles. J Phys Chem 93:5536–5540

38. Nazar MF, Khan AM, Shah SS (2009) Microemulsion system with improved loading of piroxicam: A study of microstructure, AAPS Pharm. Sci Tech In press. doi:10.1208/s12249-009-9328-9

39. Kang J, Liu Y, Xie MX, Li S, Jiang M, Wang YD (2004) Interactions of human serum albumin with chlorogenic acid and ferulic acid. Biochim Biophys Acta 1674:205–214

40. Khan SN, Islam B, Rajeswari MR, Usmani H, Khan AU (2008) Interaction of anesthetic supplement thiopental with human serum albumin. Acta Biochim Pol 55:399–409

41. Ahmad B, Parveen S, Khan RH (2006) Effect of albumin conformation on the binding of ciprofloxacin to human serum albumin: a novel approach directly assigning binding site. Biomacromolecules 7:1350–1356